Third sound on patterned substrates. II. Random arrays and classical wave localization

D. T. Smith,* C. P. Lorenson,† and R. B. Hallock
Laboratory for Low Temperature Physics, Department of Physics and Astronomy, University of Massachusetts, Amherst, Massachusetts 01003
(Received 9 March 1989)

Experiments are reported which utilize third-sound waves on thin helium films to investigate the propagation of classical waves on substrates which have been patterned with random disorder in one dimension. The results are compared with predictions due to Condat and Kirkpatrick with the conclusion that the system demonstrates classical wave localization.

I. INTRODUCTION

Wave propagation in disordered media has been of considerable interest for many years. Although work has focused primarily on electron systems,[1,2] there has also been recent work on the propagation of classical waves in disordered systems.[3–7] The interest in these systems is easily understood, very few real physical systems approximate the perfect, ordered solid assumed by Bloch in his theory of electron states, or by Debye, Brillouin, and others in their study of phonons in perfect crystals.[8]

In an effort to make progress in the understanding of wave propagation in disordered media, we have developed experiments which utilize the propagation of waves known as third sound[9–11] in thin films of superfluid helium adsorbed on substrates which are patterned[12,13] so as to allow scattering of the third-sound waves by arrays of scatterers. We have initiated our efforts in the context of one-dimensional scatterers where the effects of the disorder are strong; it is these one-dimensional experiments for the case of random arrays which are the subject of this paper. The basic techniques of third sound we have employed and the application of these techniques to periodic and quasiperiodic arrays of scatterers have been described in a previous paper.[14] We begin in Sec. II with a discussion of waves in disordered media. After a very brief review of the apparatus and technique in Sec. III, we discuss and interpret the results for the case of random arrays in Sec. IV.

II. WAVES IN DISORDERED MEDIA

Anderson[15] was the first to suggest that deviations from perfect periodicity in a solid could *fundamentally* alter the electron wave function. Prior to Anderson's work, it was thought that although electrons would scatter from impurities in a lattice and thereby lose phase coherence over length scales comparable to the mean free path between collisions, they could still be described by wave functions which extended over the entire sample as Bloch wave functions do. Anderson showed that if the disorder were strong enough, an electron wave function, $\psi(\mathbf{r})$, would become "localized;" that is, it would not be composed of extended states, but would instead have the form

$$|\psi(\mathbf{r})| \sim \exp\left[\frac{|\mathbf{r}-\mathbf{r}_0|}{\xi}\right], \tag{1}$$

where the localization length, ξ, describes the size of the region about $\mathbf{r}_0$ within which the electron is confined.

Anderson's original model of localization considered a periodic array of potential wells, with disorder introduced by assigning random depth to the wells (within some range of possible depths). The model contained one dimensionless parameter W/I, where W described the amount of disorder in the well depths, and I was the overlap integral for neighboring sites. The key question was whether the overlap of site wave functions was strong enough to produce a coherent state which extended over the entire system. Although the model could not be solved exactly, Anderson's approach indicated that there existed a critical value W_c/I below which extended states appeared. Thus, a metal-insulator transition was predicted. Shortly after Anderson's original paper, it was rigorously shown[16,17] that in one-dimensional ($d=1$) systems, electrons are always localized for any nonzero amount of disorder, although the localization length could become very long for weak disorder.[18] In three dimensions it was confirmed that there did exist a metal-insulator transition, termed the "mobility edge," which was described in terms of electron energy; electrons of energy less than a critical value were localized in a sufficiently disordered potential.[19]

Although much of the early work on localization was done on electron systems, the phenomenon of localization is a more general wave phenomenon, and many of the fundamental theoretical ideas can be applied to systems which obey the classical wave equation. This is due to the similarity between the Schrodinger equation and the classical wave equation. Classical waves are easier to study than electrons in lower-dimensional ($d \leq 2$) systems, where localization effects are strongest, because the classical wave system can be of macroscopic dimensions. In order to be an effective one-dimensional system, an electron system must have two dimensions that are small compared to the electron wavelength (~ 1 μm at 100 mK); one-dimensional classical- wave localization has been studied[3] in systems as long as 15 m. Furthermore, electron systems are complicated by electron-electron

and electron-phonon interactions.

One way to understand the phenomenon of classical wave localization is to picture a pair of two-dimensional (or three-dimensional) arrays of scattering sites (disks for $d=2$ or spheres for $d=3$), one periodic and one disordered. In the periodic array, a wave propagating from one side of the array to the other can follow many paths (scattering from site to site) through the array and arrive *coherently* at the other side. In the disordered array, on the other hand, in general, no two paths across the array will be of equal length, and no coherent propagation of the wave is possible. For the disordered array the only scattering paths which result in phase coherence are closed paths which start and end at the same location; scattering around a closed path in one direction is coherent with scattering around the *same* path in the opposite direction. This coherence for closed disordered paths is termed enhanced backscattering; the net effect is that the wave can be confined to some region of space which is characterized spatially by ξ. This enhanced backscattering has been observed directly[20] for photons incident upon random arrays of polystyrene spheres in qualitative agreement with a theoretical analysis by Stephen.[21]

In recent years, several significant advances have been made in the theoretical understanding of classical wave behavior in disordered systems. John, Sompolinsky, and Stephen[22,23] (JSS) have studied the theory of phonon localization using a field-theoretic approach first developed by Wegner[24] for electron systems. They concluded that for systems of dimensionality $d \leq 2$, all states are localized, with a localization length which increases as the frequency of the phonons decreases. For $d > 2$, they found that high-frequency phonons were localized, but that there existed a transition frequency below which the phonon states were extended. In all cases, JSS found that high-frequency phonons are localized more easily than low-frequency phonons.

Kirkpatrick[25] used a self-consistent diagrammatic technique, first developed by Vollhardt and Wölfe[26] for electron systems, to study the propagation of acoustic waves in two- and three-dimensional random arrays of hard scatterers. Although a different choice of boundary conditions at the scatterers was used, Kirkpatrick concluded, as did JSS, that for $d=2$, acoustic waves will always be localized, but that the localization length grows exponentially for both high and low frequencies, with a minimum value at some intermediate value of frequency which corresponds approximately to a wavelength equal to the radius, a of the scatterer ($\lambda \sim a$). For $d=3$, he found that extended states existed for very low and very high frequencies, but that there might exist an intermediate range of frequencies, separated from the low-frequency and high-frequency extended states by mobility edges, where states were localized for high-scatter densities.

Condat and Kirkpatrick (CK) extended the work of Kirkpatrick by studying the effects of various types of scatter boundary conditions in one dimension[27,28] and in two and three dimensions.[29,30] CK find the most interesting scattering behavior for systems with permeable scatterers,[30] i.e., scatterers which the wave can penetrate. In these systems, the scatterer cross section can be more than five times the geometrical cross section, with peaks in the cross section at various frequencies caused by resonant scattering.[31] In two dimensions, all modes are still predicted to be localized, but the localization length is expected to be a complex function of frequency, being shortest for frequencies near scatter resonant frequencies. In three dimensions, both localized and extended states are predicted. The frequency ranges within which states are localized are predicted to be complicated functions of scatterer density and the sound speed in the scatterer relative to the sound speed in the background medium.[32]

CK also predict resonant scattering effects for one-dimensional permeable-scatterer systems.[28] For $d=1$, scatterer resonances correspond to an integer number of half-wavelengths within the scatterer and lead to *increased* transmission and a divergence in the localization length at those frequencies. Such a system is shown schematically in Fig. 1 and can be realized experimentally by either layering slabs of two materials to form a quasi-one-dimensional system in three dimensions or by alternating strips on a planar surface to create a quasi-one-dimensional system in two dimensions. In Fig. 1, C_2 is the sound velocity in a scatterer, C_1 is the sound velocity in the intervening medium, and W is the width of each scatterer. The difference in sound velocities is characterized by an index of refraction $n = C_1/C_2$, with $n \geq 1$. The scatterers are placed at random, with an average spacing $\bar{l}$.

The full expression reported by Condat and Kirkpatrick[33] for the localization length ξ in a one-dimensional index-of-refraction scatter system is

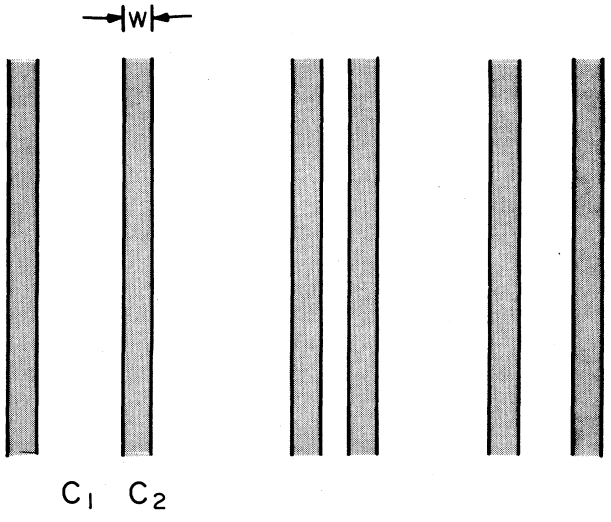

FIG. 1. Schematic representation of the substrate geometry used in the calculations of Condat and Kirkpatrick (Refs. 27 and 28). The third-sound velocities C_1 and C_2 are, in general, unequal.

$$\frac{1}{\pi}q_0\xi\arctan(q_0\xi)=\left[1+\frac{n\{4n-(n+1)^2\cos[\tilde{\eta}(n-1)]+(n-1)^2\cos[\tilde{\eta}(n+1)]\}}{(n^2-1)^2\sin^2(\tilde{\eta}n)}\right]^{-1}, \tag{2}$$

where

$$q_0=\frac{2\bar{l}(n^2-1)^2\sin^2(\tilde{\eta}n)}{4n^2+(n^2-1)^2\sin^2(\tilde{\eta}n)} \tag{3}$$

and where $\tilde{\eta}=\omega W/\tilde{C}$, $\bar{l}$ is the averaging strip spacing, W is the strip width, $\eta=\omega W/C_1$, and $\tilde{C}$ is the renormalized sound speed given by

$$\tilde{C}^2=C_1^2\left[1-\frac{2Wn\bar{l}\{(n+1)^2\sin[\eta(n-1)]+(n-1)^2\sin[\eta(n+1)]\}}{\eta[4n^2+(n^2-1)^2\sin^2(\eta n)]}\right]. \tag{4}$$

At low frequency ($\omega W/C_2\geq 1$), the localization length can be simplified to

$$\frac{\xi(\omega)}{\bar{l}}\simeq\left[\frac{C_1}{\omega W}\right]^2\frac{4}{[(C_1/C_2)^2-1]^2}. \tag{5}$$

Expression (5) will be relevant to the experimental results we will describe in Sec. IV.

Thin films of superfluid helium represent a convenient experimental system with which we may explore some of the predictions of Condat and Kirkpatrick. Such films support waves known as third sound[34] which are analogous to tidal waves on the ocean. For third sound on a smooth surface, $C=(fd\langle\rho_s\rangle/\rho)^{1/2}$ where f is the van der Waals restoring force, $\langle\rho_s\rangle/\rho$ is the effective superfluid fraction in the film and d is the helium film thickness. For thin helium films with film thickness values in the range which will be relevant to our work, the restoring force may be approximated by $f\sim 3\alpha d^{-4}$, where α is the van der Waals constant which characterizes the helium-substrate interaction.

Cohen and Machta[35] considered a two-dimensional third-sound scattering system consisting of a flat substrate with a random distribution of particles resting on it. A superfluid ^{4}He film coats both the substrate and the particles. Some excess helium is capillary condensed around the base of each particle, changing the velocity of third sound near the particle; the amount of excess fluid depends upon the film thickness far from the particle.[34] Cohen and Machta find that for such a two-dimensional system, third sound will be localized, with a frequency dependence for the localization length of the form $\xi(\omega)\propto\exp(\omega_0/\omega)^2$, where ω_0 depends upon the strength and density of scatterers. A preliminary experimental system of this type was studied in this laboratory;[36] however, the data preceded the theory and do not properly address the subsequent theoretical prediction.

Other experimental systems have previously been used to explore classical wave localization. Some of the earlier work is that of Hodges and Woodhouse;[6] more recent work is that of He and Maynard[3] and of Belzons and collaborators.[4,5] The former two groups observed localized modes in systems consisting of a taut steel wire with masses attached at positions which deviated slightly from a periodic spacing. Hodges and Woodhouse[6] placed seven masses on an 80-cm wire which was rigidly clamped at both ends; He and Maynard[3] studied 50 masses on a 15-m length of wire which was driven at one end and terminated anechoically at the other. Both experiments were able to measure the vibrational amplitude of the wire at any point along its length by placing the wire in the gap of a horseshoe-shaped magnet and measuring the induced voltage in the wire, thus allowing the eigenstates of the system to be mapped in space. For a periodic placement of the masses, both experiments showed extended states grouped by frequency into pass bands analogous to those seen in periodic electron system. For a disordered arrangement of masses, both experiments showed evidence for localized states. In the case of the work of Belzons *et al.*[4,5] evidence is seen for the localization of gravity waves in water in a one-dimensional channel with a random rough bottom.

III. HELIUM FILMS AND THE EXPERIMENTAL ENVIRONMENT

Capillary condensation of ^{4}He film on rough regions of a substrate results[37,38] in a third-sound velocity different from that seen on a smooth substrate; thus, a third-sound substrate with smooth and rough regions constitutes a system of permeable scatterers for which the index of refraction $n=C_1/C_2$ can, for appropriately chosen rough regions, be varied by changing the helium film thickness. If those scatterers are in the form of strips, as shown in Fig. 1, a quasi-one dimensional system results which constitutes an appropriate $d=1$ experimental system to test the prediction of Eq. (5). We consider the superfluid ^{4}He film to be a particularly good system to use for these studies for several reasons. First, for temperatures low enough, dissipation of third sound in the film can be very low. This is important, because the observation of localization requires that the inelastic scattering length for the sound mode be long compared to the localization length. In the experimental system studied, it was found that for $T=1.35$ K, attenuation of third sound was present but was not large enough to mask localization effects. Silicon substrates were prepared[14] with random patterns ruled according to a random number generator. To accomplish this, the smooth silicon substrate surfaces were interrupted by straight channels scribed into the surface

TABLE I. Channel-locations—first random array. Below is listing of the channel locations for the first random array studied, scaled over a range of $0 < x < 1$, followed by the relative locations of the bolometer strips. To convert these coordinates to actual positions with the array, multiply by 5 cm.

No.	x	No.	x	No.	x	No.	x	No.	x
1	0.0012	21	0.1812	41	0.4682	61	0.6066	81	0.8367
2	0.0034	22	0.1892	42	0.4741	62	0.6077	82	0.8410
3	0.0039	23	0.2019	43	0.4754	63	0.6243	83	0.8523
4	0.0073	24	0.2096	44	0.4806	64	0.6422	84	0.8794
5	0.0095	25	0.2117	45	0.4807	65	0.6423	85	0.8909
6	0.0104	26	0.2215	46	0.4864	66	0.6612	86	0.8962
7	0.0216	27	0.2235	47	0.4929	67	0.6778	87	0.8966
8	0.0549	28	0.2750	48	0.5076	68	0.6811	88	0.9024
9	0.0558	29	0.2846	49	0.5172	69	0.7078	89	0.9042
10	0.0562	30	0.2921	50	0.5229	70	0.7261	90	0.9052
11	0.0588	31	0.3190	51	0.5332	71	0.7335	91	0.9376
12	0.0735	32	0.3260	52	0.5405	72	0.7455	92	0.9386
13	0.0770	33	0.3415	53	0.5415	73	0.7696	93	0.9527
14	0.1013	34	0.3753	54	0.5567	74	0.7877	94	0.9575
15	0.1082	35	0.4011	55	0.5801	75	0.7938	95	0.9578
16	0.1098	36	0.4016	56	0.5916	76	0.7959	96	0.9663
17	0.1250	37	0.4042	57	0.5930	77	0.7998	97	0.9742
18	0.1421	38	0.4134	58	0.5955	78	0.8079	98	0.9786
19	0.1501	39	0.4198	59	0.5977	79	0.8290	99	0.9833
20	0.1668	40	0.4300	60	0.6008	80	0.8365	100	0.9974
$R4$	0.2500	$R3$	0.4500	$R2$	0.5000	$R1$	0.9200		

with a diamond tool such that 100 channels were distributed over a 5-cm length of the substrate with average spacing $\bar{l}=500$ μm. The specific locations of the various scribed channels for the random arrays we have studied are given in Table I and II. Within the rough channels, the third-sound velocity C_2 differs from that on the smooth surface C_1. To obtain data on the propagation of third sound in this system, both pulsed- and continuous-

TABLE II. Channel locations—second random array. Below is a listing of the channel locations for the second array studied, scaled over a range $0 < x < 1$, followed by the relative locations of the bolometer strips. To convert these coordinates to actual positions within the array, multiply by 5 cm.

No.	x	No.	x	No.	x	No.	x	No.	x
1	0.0080	21	0.2101	41	0.4158	61	0.5670	81	0.8484
2	0.0118	22	0.2207	42	0.4180	62	0.5701	82	0.8589
3	0.0124	23	0.2222	43	0.4251	63	0.5922	83	0.8640
4	0.0136	24	0.2316	44	0.4324	64	0.6087	84	0.8683
5	0.0328	25	0.2591	45	0.4579	65	0.6090	85	0.8780
6	0.0411	26	0.2604	46	0.4685	66	0.6164	86	0.8789
7	0.0601	27	0.2667	47	0.4699	67	0.6237	87	0.8791
8	0.0727	28	0.2698	48	0.4730	68	0.6421	88	0.8803
9	0.0827	29	0.2908	49	0.4782	69	0.6975	89	0.8897
10	0.1008	30	0.3095	50	0.5136	70	0.7201	90	0.8949
11	0.1010	31	0.3143	51	0.5263	71	0.7208	91	0.9073
12	0.1022	32	0.3162	52	0.5327	72	0.7341	92	0.9374
13	0.1105	33	0.3196	53	0.5360	73	0.7466	93	0.9456
14	0.1278	34	0.3213	54	0.5372	74	0.7550	94	0.9503
15	0.1319	35	0.3226	55	0.5375	75	0.7598	95	0.9506
16	0.1366	36	0.3259	56	0.5475	76	0.7869	96	0.9599
17	0.1536	37	0.3706	57	0.5485	77	0.7872	97	0.9604
18	0.1694	38	0.3748	58	0.5508	78	0.8229	98	0.9648
19	0.1963	39	0.3927	59	0.5512	79	0.8415	99	0.9733
20	0.2084	40	0.4138	60	0.5513	80	0.8473	100	0.9819
$R4$	0.2500	$R3$	0.4500	$R2$	0.5000	$R1$	0.9200		

wave third-sound techniques were used. Third sound was generated and detected through the use of Al strips evaporated directly on the silicon surface between selected channels. The notation for designating the drive and detector will be "$\mathcal{R}m$-$\mathcal{R}n$," where "m" designates the driver and "n" designates the detector. A more detailed discussion of the experimental techniques has been presented previously.[14]

IV. RESULTS AND DISCUSSION

The data presented here were taken on a random array $\mathcal{R}$ shown schematically in Fig. 2 by driving with a continuous sine wave at $\mathcal{R}3$ and detecting with either $\mathcal{R}2$ or $\mathcal{R}4$ using the electronics described previously.[14] The third-sound elements denoted $\mathcal{R}1$–$\mathcal{R}4$ are enumerated from left to right as seen in Fig. 2.

The $\mathcal{R}3$-$\mathcal{R}2$ spacing was $5\bar{l}$, or five times the lattice spacing, whereas the $\mathcal{R}3$-$\mathcal{R}4$ spacing was $20\bar{l}$. The third-sound amplitude as a function of frequency was measured by sweeping the drive frequency over a broad range, typically from ~10 Hz to 50 kHz. Because the third-sound drive is thermal, the third-sound frequency excited is twice the applied sine-wave frequency. All frequencies reported in this work are *third-sound* frequencies. All of the third-sound amplitudes are in arbitrary units since the third-sound detector sensitivities could not be well known for all of the coverages, temperatures, and changes of substrates encountered in the course of this work.

Figure 3 shows the received third-sound amplitude at

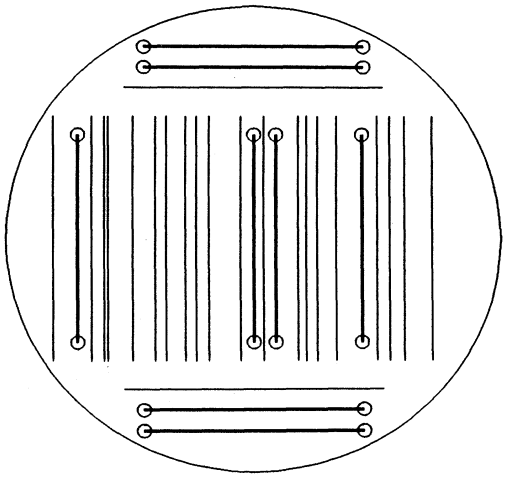

FIG. 2. Schematic representation of a random array of scribed channels in silicon. Each array used in this work contained 100 parallel channels; only 20 are schematically shown here for clarity. The channels and Al detectors shown orthogonal to the arrays were present to allow measurement of the third-sound velocity on smooth Si and to measure the reflection of third sound from a single scratch (Refs. 14 and 42).

$\mathcal{R}2$, in arbitrary units for each data set, as a function of third-sound frequency for a drive at $\mathcal{R}3$. The data were taken at the same 12 values of film thickness[39] at which a periodic array was studied.[14] The random array frequency values can be divided by the C_s (the third-sound veloc-

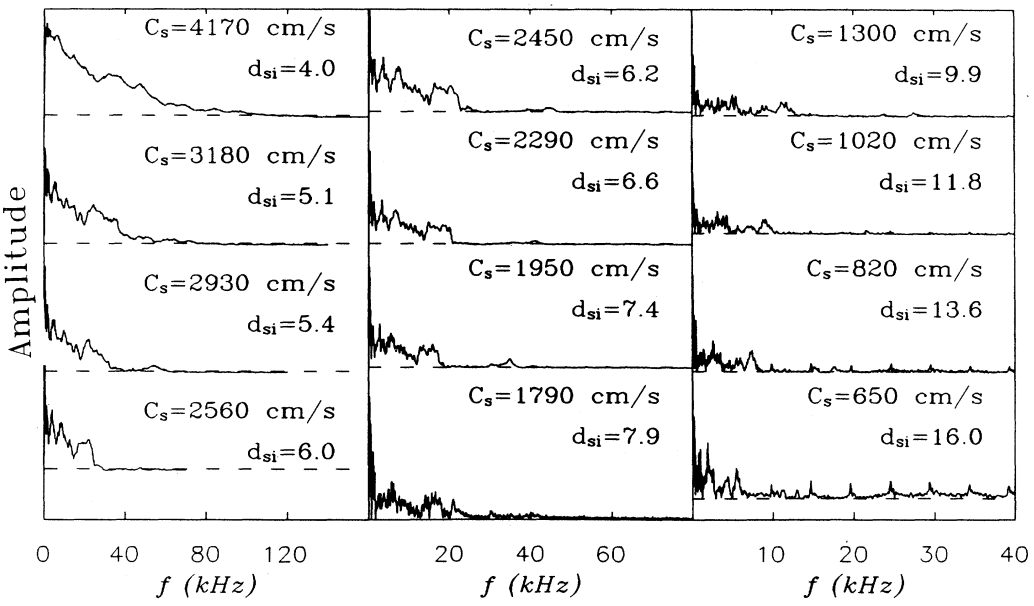

FIG. 3. Received third-sound amplitude (in arbitrary units for each subfigure) as a function of the third-sound frequency for several values of the helium film thickness. Each value of the film thickness has associated with it a different value of the (smooth silicon) third-sound velocity.

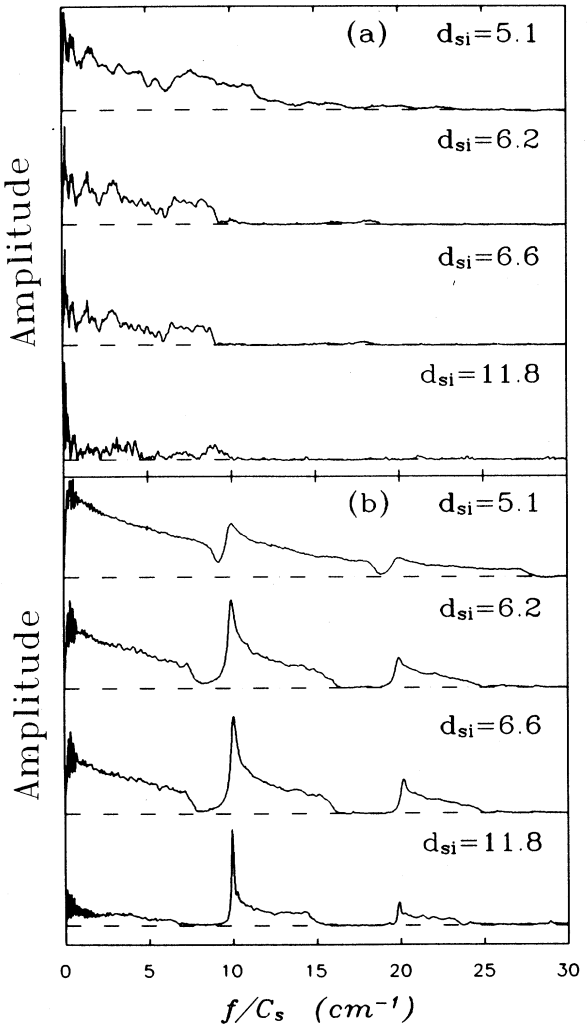

FIG. 4. Received third-sound signal as a function of wave number for the case of (a) a random array and (b) a periodic array (Ref. 14). In each case shown here, the separation between the driver and the detector was $5\bar{l}$.

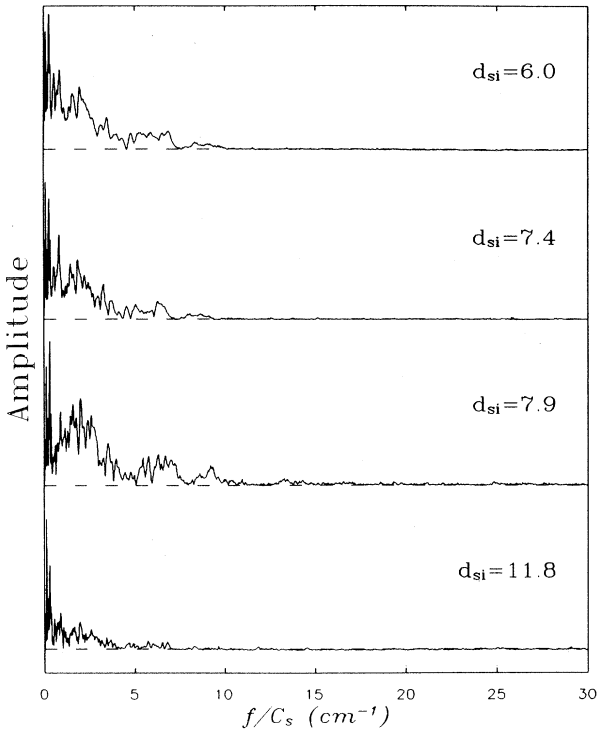

FIG. 5. Detected amplitude (in arbitrary units) at $\mathcal{R}4$ for a drive at $\mathcal{R}3$ as a function of wave number for four values of the film thickness. The dashed lines indicate zero-detected amplitude.

ity on the smooth silicon between the channels) to facilitate comparison of data taken at different coverages; this is shown for four coverages in Fig. 4(a). In comparing Fig. 4(a) to the periodic array data in Fig. 4(b), which was taken at the same coverages and over the same driver-detector separation, two differences are clear. First, the random array data do not show any of the band structure seen on the periodic array, not surprising in view of the

TABLE III. Parameters relevant to the analysis of third sound on the $\mathcal{R}$ array. Second column, third-sound velocity from time-of-flight measurements; third column, distance between driver and detector in units of $l=500$ μm; fourth column, scaling frequency determined from the fit to $I(\omega)$; fifth column, the ratio of $\bar{\omega}_5$ to $\bar{\omega}_{20}$; sixth column, $\gamma=(C_s/W\bar{\omega}_m)^2/m$, using C_s and $\bar{\omega}_m$ from the second and fourth columns; and in the seventh column, $n_\gamma=(2\gamma^{1/2}+1)^{1/2}$ calculated from the values of γ in the sixth column.

d_{si} (layers)	C_s (cm/sec)	m (l)	$\bar{\omega}_m/2\pi$ (kHz)	$\bar{\omega}_5/\bar{\omega}_{20}$	γ	n_γ
6.0	2529	5	13.9	1.9	65	4.1
		20	7.4		58	4.0
7.4	1945	5	10.3	1.9	71	4.2
		20	5.3		67	4.2
11.8	994	5	5.6	2.1	62	4.1
		20	2.7		67	4.2
16.0	646	5	3.4	1.9	71	4.2
		20	1.8		64	4.1

lack of periodicity. Second, and more significant, is the fact that although the response of the random system is comparable to the periodic system at low frequency, the random system exhibits little or no third-sound propagation for values of f/C_s greater than $\sim 10\ \mathrm{cm}^{-1}$, whereas third-sound propagates easily to $f/C_s \sim 25\ \mathrm{cm}^{-2}$ on the periodic array.

It is immediately clear that this high-frequency behavior on the random system is at least qualitatively in agreement with localization predictions; the localization length ξ is predicted to decrease with increasing frequency as $\xi \propto 1/\omega^2$. For increasing frequency if ξ changes from being longer than the driver-detector separation to being less than that separation, a significant drop in detected amplitude will be observed at higher frequencies. We will return to a more quantitative discussion of this point shortly.

Figure 5 illustrates the received third-sound amplitude at $\mathcal{R}4$ as a function of the third-sound wave vector for a third-sound drive at $\mathcal{R}3$; the driver-detector separation is $20\bar{l}$. The $\mathcal{R}3$-$\mathcal{R}2$ and $\mathcal{R}3$-$\mathcal{R}4$ low-frequency data from Figs. 4(a) and 5, respectively, are shown in Figs. 6(a) and 6(b). Careful comparison of low-frequency data from the periodic[14] and random systems shows that there are some modes common both both systems, but that there are also differences between the data from the two arrays even at very low frequencies. We believe that these low-frequency modes have their origin in the geometry of the substrates; they are drumlike modes of third sound in the entire substrate.

Because the array has only 100 scatterers, there was some concern that effects seen on the random array were particular to that specific arrangement of scatterers and not general properties of random arrays. Thus, a second random array was made by generating a second set of random positions with the constraint that the number of scatterers between each pair of strips be the same as on the periodic array. A second periodic array was made at the same time. Frequency sweeps of $\mathcal{P}3$-$\mathcal{P}2$ from this new periodic array and $\mathcal{R}3$-$\mathcal{R}2$ from the new random array for $T=1.35$ K are shown in Fig. 7 for two representative helium film coverages. Although the specific mode structure on the second random array is quite different

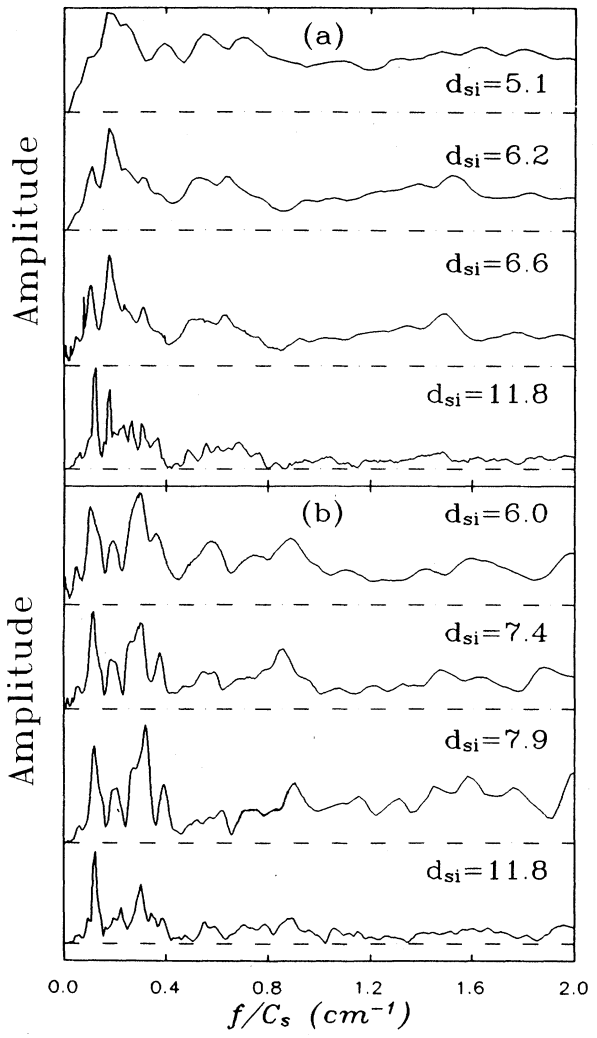

FIG. 6. Expanded view of the low-frequency data for the case of (a) $\mathcal{R}3$-$\mathcal{R}2$ and (b) $\mathcal{R}3$-$\mathcal{R}4$ driver-detector pairs. The dashed baselines are the zero-detected amplitude level.

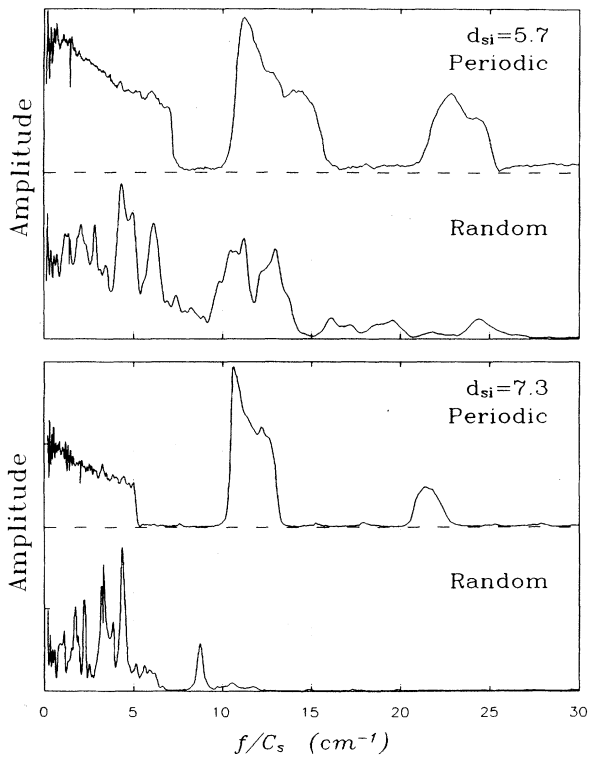

FIG. 7. Comparison of the detected amplitude (arbitrary units) for the case of periodic and random arrays for two values of the film thickness. The driver-detector pairs here were $\mathcal{P}3$-$\mathcal{P}2$ and $\mathcal{R}3$-$\mathcal{R}2$.

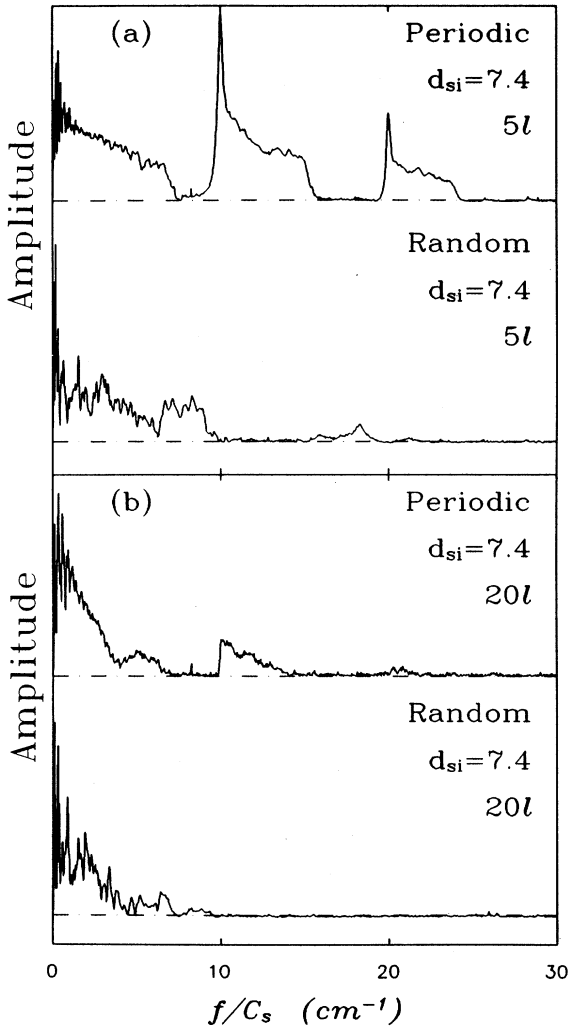

FIG. 8. Comparison of the detected amplitude (arbitrary units) for the case of two different driver-detector separations at two values of the film thickness. For the separation $5\bar{l}$ the pairs were $\mathcal{P}3$-$\mathcal{P}2$ and $\mathcal{R}3$-$\mathcal{R}2$; for $20\bar{l}$ the pairs were $\mathcal{P}3$-$\mathcal{P}4$ and $\mathcal{R}3$-$\mathcal{R}4$.

from that shown in Fig. 4 for the first random array, as would be expected for a different random arrangement of scatterers, the basic behavior is very similar; at higher coverages, there is anomalously high attenuation of high-frequency third sound. The fact that the gaps in periodic band structure seen on the second periodic array are larger than those seen on the first periodic array at comparable film thicknesses is consistent with optical measurements of the new channels which indicate that their widths ($\simeq 38$ μm) are roughly twice the width of the channels on the first arrays studied.[14]

Figure 8 shows the difference in response between the periodic and random systems for the first set of arrays at a helium film thickness of 7.4 layers; Fig. 8(a) compares periodic and random data for a driver-detector separation of $5\bar{l}$, while Fig. 8(b) does the same for a separation of $20\bar{l}$. A key difference between the periodic and random systems for both sets of arrays is the lack of high-frequency modes seen on the random array. (As mentioned earlier for the $5\bar{l}$ spacing, for example, the periodic array shows strong transmission for values of f/C_s up to almost 25 cm^{-1} (for frequencies within bands), whereas the random array shows almost no transmission for $f/C_s \geq 10$ cm^{-1}. The theory of classical wave localization presented earlier predicts just such an effect; the localization length ξ depends on frequency as $\xi \propto \omega^{-2}$ [Eq. (5)], implying that as the frequency is raised in an experiment, a drop in detected amplitude should be seen when ξ goes from being longer than the driver-detector spacing to being shorter than that spacing.)

In order to compare the data from the random array to the theoretical prediction, Eq. (5), the following analysis was performed.[13] First, we make the assumption that the third-sound amplitude, a distance $m\bar{l}$ from the driver, $A_m(\omega)$, scales with a single, m-dependent frequency $\bar{\omega}_m(d)$, i.e., $A_m(\omega)=g(\omega/\bar{\omega}_m)$. It then follows that

$$I_m(\omega)=\int_0^{\omega} A_m(\omega)d\omega=\bar{\omega}_m G(\omega/\bar{\omega}_m)\ ,$$

such that $I_m(\omega)/\bar{\omega}_m$ is a universal function of $\omega/\bar{\omega}_m$. A value for $\bar{\omega}_m$ can then be extracted from the integrated data by fitting it to an exponential function, $I_F(\omega)$. We

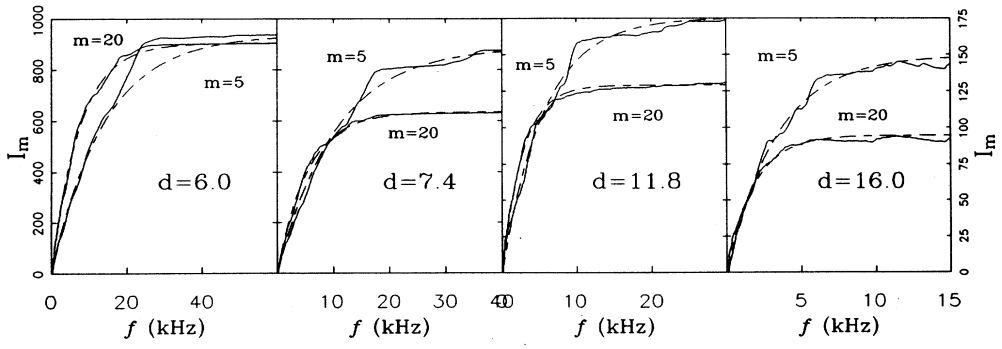

FIG. 9. Integral of the $\mathcal{R}3$-$\mathcal{R}2$ ($m=5$) and $\mathcal{R}3$-$\mathcal{R}4$ ($m=20$) data (in arbitrary but relative units) at several values of the helium film thickness. The dashed lines are fits to the integrals using the functional form for I_F given in the text.

have chosen the convenient form

$$I_F(\omega)=B_m[1-\exp(\omega/\bar{\omega}_m)] ,$$

and obtained $\bar{\omega}_m$ for $m=5$ ($\mathcal{R}3$-$\mathcal{R}2$) and $m=20$ ($\mathcal{R}3$-$\mathcal{R}4$) at several values of the helium film thickness. If Eq. (5) holds for this system, then the observed values for $\bar{\omega}_m$ should scale as $\bar{\omega}_m \propto 1/\sqrt{m}$.

One small correction needed to be applied to each data set before the above analysis could be carried out. The exponential function used to fit the integrated data assumes that the detected third-sound amplitude drops to zero for ω large, so that the integral will level off at a fixed value B_m. In fact, because of small background noise levels and dc offsets in instrumentation (and in some cases vapor sound resonances[40] at high frequency), the highest-frequency data do not always have an average amplitude of zero and the integral asymptotes to a straight line whose slope is typically not quite zero. To overcome this, a fit is made to the expression

$$I_m=B_m[1-\exp(\omega/\bar{\omega}_m)]+C_m\omega$$

instead of $I_F(\omega)$ and the linear term is subtracted from the integrated data so that the integral does approach a fixed value of B_m for large ω.

Figure 9 shows the resulting integrated data for $m=5$ and 20 at four values of film thickness along with fits to

$$I_F(\omega)=B_m[1-\exp(\omega/\bar{\omega}_m)] .$$

In each of the cases shown the relative amplitudes among the various figures are arbitrary. Table III shows the values of $\bar{\omega}_m$ obtained from these fits. Note that the values for $\bar{\omega}_m$ are consistent with $1/\sqrt{m}$ scaling; that is $\bar{\omega}_5/\bar{\omega}_{20}\simeq\sqrt{20/5}=2$. If $\bar{\omega}_m$ is taken to be the frequency for which $\xi(\bar{\omega}_m)=m\bar{l}$, then Eq. (5) can be used to estimate the value of n at each coverage as follows:

$$\frac{\xi(\omega)}{\bar{l}}=\left[\frac{C_s}{\omega W}\right]^2\frac{4}{(n^2-1)^2} ,$$

$$\frac{\xi(\bar{\omega}_m)}{m\bar{l}}=1=\frac{1}{m}\left[\frac{C_s}{\bar{\omega}_m W}\right]^2\frac{4}{(n^2-1)^2} , \tag{6}$$

$$\gamma\equiv\frac{1}{m}\left[\frac{C_s}{\bar{\omega}_m W}\right]^2=\frac{(n^2-1)^2}{4} .$$

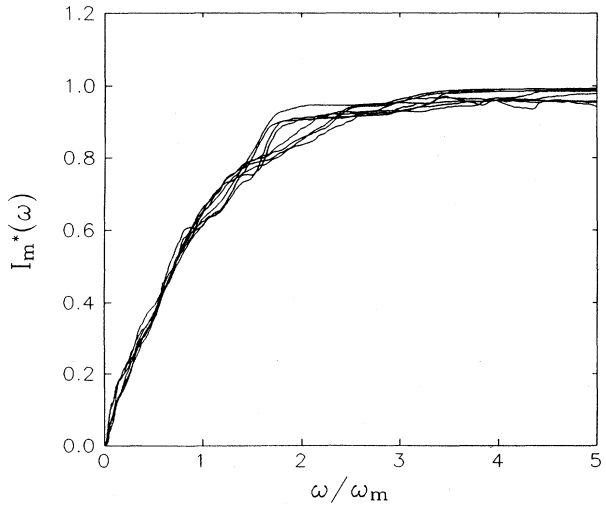

FIG. 10. Data from Fig. 9 which show the universal behavior of the random system. Amplitudes have been normalized with the values of B_m obtained from fits to each integral and the frequencies have been scaled by the values of $\bar{\omega}_m$ obtained from those same fits.

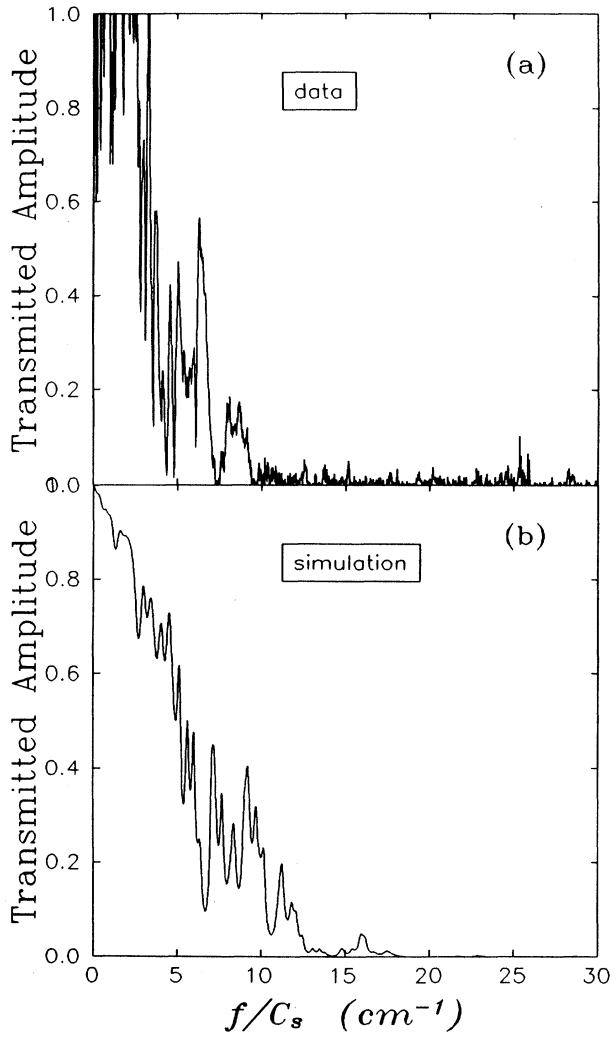

FIG. 11. Comparison of (a) detected third-sound amplitude for the case of $m=20$ for a film thickness of 7.4 layers and (b) a simulation of the transmitted amplitude with attenuation and site disorder taken into account in the calculation. For the simulation the attenuation was of the form $\exp^{-\delta\omega}$ with $\delta=2.,5\times10^5/s$. The site disorder was of the form $n=3.5+\Delta n$, with Δn picked at random from the range $-1\le\Delta n\le1$.

The parameter $\gamma=(C_s/\bar{\omega}_m W)^2/m$ is given in the sixth column of Table III for each set of data analyzed, and an index n_γ is calculated using $\gamma=(n_\gamma^2-1)^2/4$, as shown in the last column. Values for the index calculated in this way are slightly higher than those obtained from detailed studies of the band structure of third sound on substrates patterned with periodic arrays,[14] but not substantially so. Values for γ are slightly lower for $d_{si}=6.0$ layers than for the other coverages in Table III, in qualitative agreement with the band-structure results,[14] although at 6.0 layers $n_\gamma \simeq 4.0$ is significantly higher than the value for the index determined from the periodic band structure.

The data $I_m(\omega)$ from Fig. 9 can be scaled by normalizing the amplitude with the fit values B_m ($I_m^* \equiv I_m/B_m$), so that the integrated data all asymptote to 1.0 for high frequencies, and the frequency can be scaled by $\bar{\omega}_m$. Figure 10 shows the data from all eight curves in Fig. 9 with the scaling; it is clear that $I_m^*(\omega)$ is indeed a universal function of $\omega/\bar{\omega}_m$.

Because both a separate study of smooth silicon wafers[14] and a simulation of the periodic system indicated that there is some frequency-dependent third-sound attenuation present in these systems, it is important to address the issue of whether this attenuation could be responsible for he general frequency response observed on the random array, and, in particular, the observed scaling of $\bar{\omega}_m$ as $1/\sqrt{m}$. The first observation which argues against attenuation being a significant factor in the analysis is a simple comparison of the data from the random and periodic arrays, as shown in Figs. 8(a) and 8(b). Attenuation effects (and variations in n among the strips) are common to both the periodic and random systems, yet many more high-frequency modes extend from driver to detector on the periodic array than on the random array. That is, although there is a decay in amplitude with increasing frequency in both systems, the characteristic frequency of that decay in the periodic system is much higher than that in the random system. The only difference between those systems is the positional disorder in the scatterer locations deliberately introduced on the random substrate.

A more quantitative argument against attenuation seriously affecting the conclusion that the random system exhibits localization comes from simulations[41] of the random array. In analysis of periodic array data,[14] it was found that an overall decay in amplitude with increasing frequency was consistent with a frequency-dependent attenuation of the form $\exp^{-\delta_m \omega}$ for transmission through an m-channel array. As an example, in Fig. 11 we illustrate for the case of a $d=7.4$ layer helium film a simulation (analogous to simulations carried out earlier[14] for periodic arrays) of a 20-channel random array, using the same values of attenuation ($\delta_{20}=2.5\times10^5$), site disorder ($-1\le\Delta n\le 1$), average index of refraction (3.5), and C_s (2000 cm/s) as were used in the periodic array analysis[14] for the $d=7.4$ layer case. Data from the random array for $m=20$ and $C_s\simeq 2000$ cm/s is also shown (the $d=7.4$ layer data from Fig. 5); the simulation and data are in good qualitative agreement.

It should be pointed out that the attenuation used in the simulations cannot, by itself, explain the sharp drop in the response of the random system at higher frequencies. The characteristic frequencies of the attenuation (the frequencies at which the amplitude has dropped to $1/e$ of its dc value) are 200 kHz for $m=5$ and 40 kHz for $m=20$. By comparison, Table II shows that for $d=7.4$ layers ($C_s\simeq 2000$ cm/s), the random array data has characteristic frequencies of $\bar{\omega}_5/2\pi=10.3$ kHz and $\bar{\omega}_{20}/2\pi=5.3$ kHz. If 5.3 kHz ($\delta=3.3\times10^4$/s) is used as the characteristic attenuation frequency in a 20-scatterer random array simulation,[41] the result, shown in Fig. 12, looks nothing like the random array data. Referring back to the data of Fig. 3, it is seen that the random data have many sharp, jagged features including minima, even at low frequency, where the amplitude goes to zero. These minima are the result of interference from waves scattered from many sites, and the introduction of attenuation strong enough to account for the $\bar{\omega}$ seen on the random array completely destroys this "ragged" appearance in simulations. Consequently, although there clearly is attentuation present in this system, it alone cannot explain our observations, and thus it does not affect the basic conclusion that this random system does, in fact, demonstrate classical wave localization.

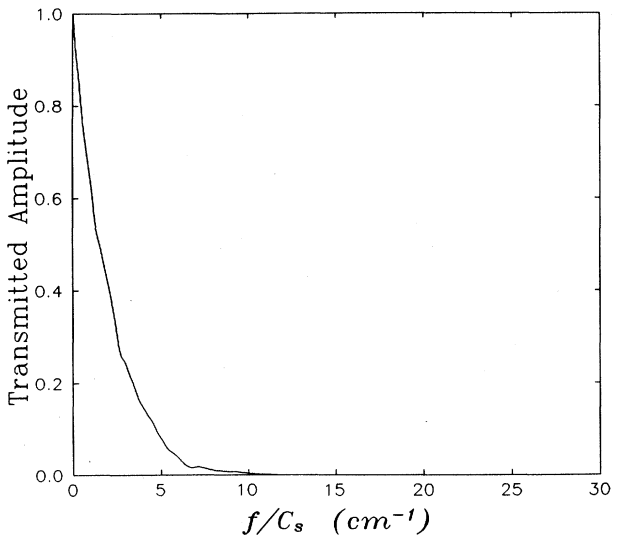

FIG. 12. Simulation of the transmitted amplitude through a 20-element random array of the case of site disorder and strong attenuation. Attenuation was of the form $\exp^{-\delta\omega}$ with $\delta=3.4\times10^4$/s. The site disorder was of the form $n=3.5+\Delta n$, with Δn picked at random from the range $-1\le\Delta n\le 1$.

V. SUMMARY

Third-sound propagation has been studied on disordered substrates in one dimension. Good experimental agreement is found between the data for substrates ruled with random disorder and the theory of Condat and Kirkpatrick for the function form of the localization length for a one-dimensional system of scatterers. Thus,

we conclude that classical wave localization is observed as expected in this system.

ACKNOWLEDGMENTS

We thank K. R. McCall and R. A. Guyer for extensive discussions and guidance with a number of aspects of the analysis carried out here. We have benefited from discussions with C. Condat, J. Machta, and P. Sheng concerning various aspects of classical wave localization. R. Verner of the Physics and Astronomy machine shop suggested the machine tool arrangement and produced the scribed substrates. This work was supported by the National Science Foundation primarily through Grant No. DMR 85-17939 and to a lesser extent by Grant No. DMR 88-20517.

*Current address: National Institute of Standards and Technology, Gaithersburg, MD 20899.

†Current address: Alcan International Ltd., Kingston, Ontario, Canada.

[1]G. J. Dolan, J. C. Licini, and D. J. Biship, Phys. Rev. Lett. **57**, 138 (1986).

[2]See, for examples of reviews in this area, P. A. Lee and T. V. Ramakrishnan, Rev. Mod. Phys. **57**, 287 (1985); G. Bergmann, Phys. Rep. **107**, 1 (1984).

[3]S. He and J. D. Maynard, Phys. Rev. Lett. **57**, 3171 (1986).

[4]M. Belzons, P. Devillard, F. Dunlop, E. Guazelli, O. Parodi, and B. Souillard, Europhys. Lett. **4**, 909 (1987).

[5]M. Belzons, E. Guazzelli, and O. Parodi, J. Fluid Mech. **186**, 539 (1988).

[6]C. H. Hodges and J. Woodhouse, J. Acoust. Soc. Am. **74**, 894 (1983).

[7]For an earlier review of wave propagation in random media, see, for example, A. Ishimaru, *Wave Propagation and Scattering in a Random Media* (Academic, New York, 1978), Vols. 1 and 2.

[8]See, for example, C. Kittel, *Introduction to Solid State Physics* (Wiley, New York, 1976), Chaps. 4, 5, and 7.

[9]K. R. Atkins, Phys. Rev. **113**, 962 (1959).

[10]K. R. Atkins and I. Rudnick, in *Progress in Low Temperature Physics,* edited by C. J. Gorter (North-Holland, Amsterdam, 1970), Vol. 6.

[11]J. S. Brooks, F. M. Ellis, and R. B. Hallock, Phys. Rev. Lett. **40**, 240 (1978).

[12]D. T. Smith, C. P. Lorenson, and R. B. Hallock, Bull. Am. Phys. Soc. **32**, 1106 (1987); **33**, 382 (1988).

[13]D. T. Smith, C. P. Lorenson, R. B. Hallock, K. R. McCall, and R. A. Guyer, Phys. Rev. Lett. **61**, 1286 (1988).

[14]D. T. Smith, C. P. Lorenson, and R. B. Hallock, Phys. Rev. B **40**, 6634 (1989).

[15]P. W. Anderson, Phys. Rev. **109**, 1492 (1958).

[16]N. F. Mott and W. D. Twose, Adv. Phys. **10**, 107 (1961).

[17]R. E. Borland, Proc. R. Soc. London Ser. A **274**, 529 (1963).

[18]For a review of localization theory prior to the introduction of scaling theory, see D. J. Thouless, in *Ill-Condensed Matter,* edited by G. Toulous and R. Balian (North-Holland, Amsterdam, 1979), p. 1; N. F. Mott and E. A. Davis, *Electronic Processes in Non-Crystalline Materials* (Clarendon, Oxford, 1979).

[19]N. F. Mott, Adv. Phys. **16**, 49 (1967).

[20]M. P. Van Albada and A. Lagendijk, Phys. Rev. Lett. **55**, 2692 (1985); P. E. Wolf and G. Maret, *ibid.* **55**, 2696 (1985).

[21]M. J. Stephen, Phys. Rev. Lett. **56**, 1809 (1986).

[22]S. John, H. Sompolinsky, and M. J. Stephen, Phys. Rev. B **27**, 5592 (1983).

[23]S. John, Phys. Rev. B **31**, 304 (1985).

[24]F. J. Wegner, Z. Phys. B **35**, 207 (1979).

[25]T. R. Kirkpatrick, Phys. Rev. B **31**, 5746 (1985).

[26]D. Vollhardt and P. Wölfle, Phys. Rev. Lett. **45**, 842 (1980); Phys. Rev. B **22**, 4666 (1980).

[27]C. A. Condat and T. R. Kirkpatrick, Phys. Rev. B **32**, 495 (1985).

[28]C. A. Condat and T. R. Kirkpatrick, Phys. Rev. B **33**, 3102 (1986).

[29]C. A. Condat and T. R. Kirkpatrick, Phys. Rev. Lett. **58**, 226 (1987).

[30]C. A. Condat and T. R. Kirkpatrick, Phys. Rev. B **36**, 6782 (1987).

[31]In order for these resonances to be observed all scatterers must be of the same with respect to size and internal sound velocity; i.e., they must all have the same resonance frequencies.

[32]P. Sheng and Z. Q. Zhang [Phys. Rev. Lett. **57**, 1879 (1986)] have also studied the theory of $d=3$ acoustic wave localization.

[33]C. A. Condat and T. R. Kirkpatrick, Phys. Rev. B **33**, 3102 (1986); C. A. Condat (private communication).

[34]See, for example, S. Putterman, *Superfluid Hydrodynamics* (North-Holland, Amsterdam, 1974).

[35]S. M. Cohen and J. Machta, Phys. Rev. Lett. **54**, 2242 (1985).

[36]D. T. Smith, M. Liebl, M. D. Bummer, and R. B. Hallock, in *Proceedings of the 17th International Conference on Low Temperature Physics,* edited by V. Eckern *et al.* (North-Holland, Amsterdam, 1984).

[37]M. Z. Shoushtari and K. L. Telschow, Phys. Rev. B **26**, 4917 (1982).

[38]D. T. Smith and R. B. Hallock, Phys. Rev. B **34**, 226 (1986).

[39]Values of the film thickness reported in this work are obtained from the assumed values of the van der Waals constant of 27 and 36 (layers)^3 K for glass and silicon, respectively. The silicon value was determined by reference to the glass value (Ref. 38).

[40]It is possible to generate sound waves in the helium vapor by means of the third-sound generators on the substrate. The efficiency of this process is a function of the temperature and the thickness of the helium film.

[41]Simulations of the type we describe here were first applied to this system by K. R. McCall and R. A. Guyer, Bull. Am. Phys. Soc. **30**, 806 (1988); (private communication).

[42]The reflection of third sound from scratches and the edges of substrates is commonly seen and is relatively well known; see, for a recent example, E. R. Generazio and R. W. Reed, J. Low Temp. Phys. **56**, 355 (1984).